Research article

Drug Testing and Analysis

Received: 17 June 2011 Revised: 19 August 2011 Accepted: 28 August 2011 Published online in Wiley Online Library

(wileyonlinelibrary.com) DOI 10.1002/dta.365

Development of liquid chromatography-tandem mass spectrometry-based analytical assays for the determination of HIF stabilizers in preventive doping research

Simon Beuck,[a] Wolfgang Bornatsch,[b] Andreas Lagojda,[b] Wilhelm Schänzer[a] and Mario Thevis[a]*

Hypoxia-inducible factor (HIF) stabilizers increase blood haemoglobin levels after oral administration and their use in sports was recently banned by the World Anti-Doping Agency. For the support of analytical assay development, the metabolic fate of two model HIF stabilizers, based on the isoquinoline-3-carboxamide scaffold of the lead drug candidate FG-2216, was assessed by *in vitro* methods. The analytes were identified and characterized by liquid chromatography-tandem mass spectrometry (LC-MS/MS) in positive and negative ionization mode using an API 4000 Qtrap as well as an exactive high resolution-high accuracy MS. The model HIF stabilizer N-[(1-chloro-4-hydroxy-7-isopropoxy-isoquinolin-3-carbonyl)-amino]-acetic acid (1), was converted into 3 major phase I metabolites by hydroxylation, dealkylation, and dehydrogenation. The structures of the hydroxylated and the dealkylated metabolites were confirmed by LC-coupled nuclear magnetic resonance spectroscopy. Moreover, glucuronic acid conjugates of the active drug and one of the dealkylated phase I metabolite were identified. Hydroxylation of model compound 2 (N-[(1-chloro-4-hydroxy-isoquinolin-3-carbonyl)-amino]-acetic acid) yielded two metabolites, regioisomeric to the dealkylated product of 1. Mass spectral data of compounds 1 and 2, as well as a structure-related analogue were included into a multi-target analytical assay based on direct injection and LC-MS/MS analysis of human urine. The method was validated for quantitative purposes. In an approach of preventive doping research, more comprehensive screening methods applying precursor ion (*m/z* 166) and neutral loss (-10 Da) scans were developed, allowing for the detection of unknown metabolites and structurally analogous HIF stabilizers emerging from ongoing lead structure developments. Copyright © 2011 John Wiley & Sons, Ltd.

Keywords: HIF stabilizers; preventive doping research; *in vitro* metabolism; LC-MS/MS; neutral loss scan

Introduction

Stabilizers of the hypoxia-inducible factor (HIF) belong to a class of pharmacologically active, investigational substances that are capable of inducing the endogenous erythropoietic system.[1,2] They have been shown to significantly increase blood haemoglobin levels after oral administration and are proposed to serve as potential substitutes for the injection of human recombinant erythropoietin (EPO) in the treatment of anaemic disorders.[3,4] The small molecule drug candidates act as inhibitors of the HIF-specific prolyl hydroxylase domain-containing proteins (PHD), that regulate the oxygen-dependent stability of the transcription factor.[5] HIF stabilizers are therefore synonymously termed HIF-PHD inhibitors (HIF-PHI). Due to the increased capacity for oxygen transport and the potentially performance-enhancing effect, the use of HIF stabilizers in sports has been explicitly banned according to the latest 2011 Prohibited List published by the World Anti-Doping Agency (WADA).[6]

To date, no clinically approved PHD inhibitor for the stabilization of the hypoxia-inducible factor is available on the market but several drug candidates are currently under investigation in clinical trials. An overview over recently claimed patents is given by Yan *et al.*[7] FibroGen Inc. (San Francisco, CA, USA) in cooperation with Astellas Pharma Inc. (Tokyo, Japan) has taken a lead position in the clinical development of PHD inhibitors and their first drug candidate FG-2216 (Astellas code name YM 311) has completed phase II clinical trials in the USA.[7] A second, potentially structure-related drug candidate termed FG-4592 has recently entered phase IIb clinical trials in the USA[8] and is also developed in Japan, Europe, Commonwealth of Independent States (CIS), Middle East, and South Africa by Astellas Pharma under the code name ASP-1517.[9] The molecular structures of the drug candidates have not yet been officially disclosed but a growing body of evidence indicates a core structure consisting of a 4-hydroxy-isoquinoline-3-carboxamide scaffold (Figure 1).[10,11] Compound **2** ([(1-chloro-4-hydroxy-isoquinoline-3-carbonyl)-amino]-acetic acid; Figure 1) seems to be the most likely candidate corresponding to FG-2216.[7] In a patent from 2006, oral administration of this compound was claimed to increase serum

* *Correspondence to: Mario Thevis, PhD, Institute of Biochemistry – Center for Preventive Doping Research, German Sport University Cologne, Am Sportpark Müngersdorf 6, 50933 Cologne, Germany. E-mail: m.thevis@biochem.dshs-koeln.de*

a *Institute of Biochemistry – Centre for Preventive Doping Research, German Sport University Cologne, Am Sportpark Müngersdorf 6, 50933 Cologne, Germany*

b *Bayer CropScience AG, Alfred-Nobel-Str. 50, 40789 Monheim, Germany*

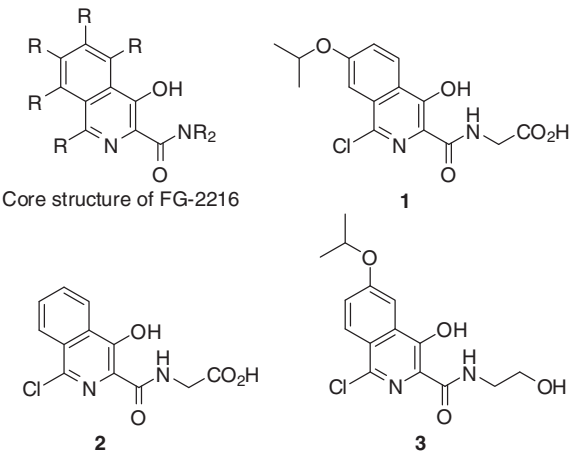

Figure 1. Proposed core structure of FG-2216 and structures of investigated model HIF stabilizers **1–3**.

EPO levels of healthy human subjects in a dose dependent manner by acting as a 2-oxoglutarate mimetic.[12]

In order to comply with the recent explicit prohibition of these substances by WADA, the timely development of analytical assays is required. In the course of preventive doping research, compounds **1–3** (Figure 1) were synthesized as model HIF stabilizers and fully characterized by electrospray ionization (ESI) high resolution-high accuracy tandem mass spectrometry (MS^n) in previous studies.[13,14]

Here, the metabolic fate of HIF stabilizer **1**, serving as a model compound for a set of isoquinoline-3-carboxamide-based HIF stabilizers, was investigated by *in vitro* methods and liquid chromatography electrospray ionization (tandem) mass spectrometry (LC-ESI-(MS/)MS) in positive and negative ion mode, as well as LC-coupled nuclear magnetic resonance spectroscopy (LC-NMR). The results were compared to the metabolites formed in an *in vitro* assay of model HIF stabilizer **2**. The characterized *in vitro* metabolites can potentially serve as target analytes for urinary doping control analysis. Moreover, the mass spectral data of intact compounds **1–3** were included into a novel multi-target detection assay used for routine doping control.[15] It is based on direct injection of human urine and simultaneous LC-ESI-MS/MS determination of protonated and deprotonated compounds with scan-to-scan polarity switching. Besides the targeted detection of model compounds **1-3**, characteristic mass spectrometric features of this class of compounds were used for the development of comprehensive urinalysis assays based on precursor ion and neutral loss scans, capable of identifying a wide range of structural analogues and unknown metabolites of isoquinoline-3-carboxamide-based HIF stabilizers.

Materials and methods

Chemicals and reagents

All target compounds as well as the $^{13}C_8$-^{15}N-labelled carboxy metabolite of the synthetic cannabinoid JWH-018 (internal standard) were synthesized and fully characterized as previously described.[13,14,16] Human liver microsomal and S9 enzymes were purchased from BD Gentest (Woburn, MA, USA), nicotinamide adenine dinucleotide phosphate (NADPH) and ß-glucuronidase (*E.coli*) from Roche Diagnostics (Mannheim, Germany), adenosine-3′-phosphate-5′-phosphosulfate (PAPS) from Calbiochem/EMD Biosciences Inc. (La Jolla, CA, USA), D-saccharic-acid-1,4-lactone and uridine-5′-diphosphoglucuronic acid (UDPGA) from Sigma Aldrich (Deisendorf, Germany). MiliQ water was used for all aqueous buffers and all organic solvents (Merck, Darmstadt, Germany) and reagents were of analytical grade.

In vitro assay for metabolic reactions

According to earlier protocols,[17] *in vitro* metabolic reactions of model HIF stabilizers were conducted with human liver S9 and microsomal fractions (2 mg/ml final protein concentration) and 100 μM analyte concentration in a 50 mM phosphate buffer at pH 7.4, containing $MgCl_2$ and the glucuronidase inhibitor 1,4-sacharic acid lactone (both 5 mM). For differentiation of metabolic versus non-metabolic reactions, different blank samples were prepared with each batch of incubation, for example, a substrate blank, a co-factor blank, and an enzyme blank. Phase I metabolism was initiated by addition of NADPH (5 mM) as co-factor and incubation at 37 °C. For phase II conjugation reactions, the co-factors UDPGA (10 mM) for glucuronidation and PAPS (80 μM) for sulfonation were added after 1 h and the incubation was continued for additional 2 h. Metabolic reactions were stopped by adding 200 μL of ice-cold acetone and the (protein) precipitate removed by centrifugation at 17 000 x *g* and 4 °C for 5 min. The supernatant was transferred to a fresh test tube and the acetone removed in a vacuum centrifuge. After another centrifugation at 17 000 x *g* for 5 min, the supernatant was diluted by 1:5 with 2% aqueous acetic acid before direct analysis by LC-ESI-(MS/)MS.

Liquid chromatography-tandem mass spectrometry

The analytical system for the initial screening for potential metabolites consisted of an Agilent 1100 Series high-performance liquid chromatograph (Agilent Technologies, Waldbronn, Germany) interfaced to an API 4000 QTrap mass spectrometer (AB Sciex, Darmstadt, Germany) using electrospray ionization in positive and negative ion mode aiming at the detection of both protonated and deprotonated analytes, respectively. Extracted ion chromatograms of a Q1 full scan analysis were used for initial screening. Suspicious signals were further characterized by tandem mass spectrometry (enhanced product ion scan (EPI), multiple reaction monitoring (MRM), or MS^3 experiments). The source temperature was set to 500 °C and the spray voltages to 5500 V and −4200 V in positive and negative ion mode, respectively. Collision gas was nitrogen (5×10^{-3} Pa) delivered by a nitrogen generator (CMC Instruments, Eschborn, Germany). The separation of analytes was achieved on a Hypersil Gold C_{18} analytical column (2.1×50 mm, 1.9 μm particle size, Thermo Fisher Scientific, Bremen, Gemany) using 5 mM ammonium acetate buffer at pH 3.5 and acetonitrile as mobile phases A and B, respectively. The gradient using a 300 μl/min flow rate was programmed as follows: 95% A (0.5 min); 95% A -> 50% A (6 min), 50% A (2 min), 50% A -> 30% A (2 min), 0% A (2 min), 95% A (2 min at 500 μl/min, 2 min at 300 μl/min).

For the determination of elemental compositions of potential metabolites and their product ions, LC-high resolution-high accuracy mass spectrometry analysis was conducted using a Thermo Accela LC coupled to an Exactive mass spectrometer (Thermo, Bremen, Germany). The analytical column was the same as described above, while the solvents consisted of 0.1% formic acid (A) and acetonitrile containing 0.1% formic acid (B). The flow rate

was set to 250 µl/min and the percentage of A was gradually decreased from 95% to 0% in 8 min, followed by elution at 100% B for 2 min and re-equilibration at 95% A for 5 min (total runtime 15 min). MS data were recorded in positive and negative ionization mode with scan-to-scan polarity switching using (i) full scan from *m/z* 100–700 at a resolution of 50 000 (full width at half maximum) (ii) full scan from *m/z* 70–700 with higher-energy collision-induced dissociation (HCD) set to 20 V and −20 V and (iii) full scan from *m/z* 70–700 with HCD at 50 V and −50 V and resolution set to 25,000, respectively. The capillary voltages were 4.5/-4.5 kV and the capillary temperature was maintained at 275 °C. Nitrogen was used as collision gas in the HCD cell.

Liquid chromatography nuclear magnetic resonance spectroscopy

The proposed structures derived from the mass spectrometric studies were confirmed using LC-NMR analysis[18] of *in vitro* synthesized metabolites. For this purpose, a larger *in vitro* metabolism batch was prepared by incubation of 300 µM of **1** in an assay volume of 10 ml (the composition of all other components was the same as described above). After protein precipitation (*vide supra*), the metabolites were extracted from the aqueous solution by liquid-liquid extraction (LLE) with ethyl acetate at pH 5 and the organic solvent was evaporated under reduced pressure. The residue was resuspended in 5 ml of a K_2CO_3/$KHCO_3$-buffer (pH 11) and further impurities were extracted with ethyl acetate. The remaining aqueous solution was brought to pH 5 with glacial acetic acid, followed by solid phase extraction on Oasis HLB cartridges (200 mg/6 ml) and methanol elution. Evaporation of the solvent yielded 2.1 mg of pre-cleaned mixture of metabolites. Finally, 144 µg of this product were introduced into the LC-MS-SPE-NMR system using an injection volume of 10 µl of methanol. The instrumental LC-setup consisted of an Agilent 1100 Series HPLC (Waldbronn, Germany) furnished with a Macherey-Nagel Nucleodur C_{18} Gravity column (250×2 mm, particle size 5 µm, Düren, Germany). The analytes were separated using gradient elution with 0.1% formic acid as solvent A and acetonitrile fortified with 0.1% of formic acid as solvent B. The LC-run was conducted with a 300 µl/min flow rate and started with 1 min of isocratic elution at 5% B and the gradient was linearly increased to 95% B in 25 min. After maintaining this solvent composition for 10 min, re-equilibration of the column was initiated. A post-column split diverted the flow to a UV detector and an Esquire 3000 plus mass spectrometer (Bruker Daltonics, Bremen, Germany), which detected the analytes as protonated molecules and served as trigger for the online-SPE unit (Spark, AJ Emmen, the Netherlands), binding the target substances on a Hysphere Resin GP (10–12 µm, Spark). After drying under a nitrogen stream, the analytes were eluted into the NMR probe using 200 µl of CD_3OD and NMR spectra (^1H, ^1H-^1H COSY, HSQC) were recorded on a Bruker AV 600 spectrometer (Bruker, Karlsruhe, Germany) at room temperature. The solvent residual signal served as reference peak for calibration of the spectra.

Routine LC-MS/MS analysis

For urine analysis, 190 µl of urine were fortified with 10 µl of a solution of $^{13}C_8$-^{15}N-carboxy-JWH-018[16] (1 µg/ml) as internal standard (final concentration of 50 ng/ml) and the resulting mixture was centrifuged at 17 000 × *g* for 5 min prior to direct injection of 5 µl of the sample for LC-ESI-MS/MS analysis. The analytical system consisted of an Agilent 1100 Series high-performance liquid chromatograph (Agilent Technologies, Waldbronn, Germany) coupled to an API 5500 QTrap mass spectrometer (AB Sciex, Darmstadt, Germany), in order to allow for the simultaneous MRM-detection of protonated and deprotonated analytes using electrospray ionization with scan-to-scan polarity switching.[15] The basic settings were the same as described for the initial metabolite screening by API 4000 QTrap MS.

The routine screening employed a Macherey Nagel Nucleodur C_{18} Pyramid analytical column (2.1×50 mm, 3 µm particle size) with a Phenomenex Gemini C_6-Phenyl precolumn (4x2 mm) for the separation of analytes. The gradient elution, using a 350 µl/min flow rate and the same solvents as described for the API 4000 QTrap system, started at 100% A and was linearly increased to 10% A in 4.1 min. The flow rate was increased to 500 µl/min and the solvent composition switched to 100% A in 0.4 min, followed by re-equilibration for 6 min at 500 µl/min and for 0.25 min at 350 µl/min (total runtime 10.75 min). Where reference material was available, the MS parameters for MRM detection were tuned for each compound by direct infusion of analyte solution (500 ng/ml in acetonitrile/formic acid 0.5%, 1:1). The settings for the deprotonated analytes **1–3** are summarized in Table 1.

Method validation

Linearity

The linearity of the method was tested by analyzing urine samples fortified with 2, 10, 40, 100, 150, and 200 ng/ml of analyte mix, respectively, with six replicates at each concentration level. The mean peak area ratios of analyte and internal standard were plotted against the nominal concentrations.

Stability of analytes

The stability of the analytes in urine matrix was investigated by storing spiked (analyte mix of 50 ng/ml) urine samples with at

Table 1. MS settings for the detection of compounds **1–3** and the internal standard (**ISTD**) by +/− MRM using the API 5500 QTrap MS system

Comp.	Pos. MRM	DP [V]	CE [V]	CXP [V]	Neg. MRM	DP [V]	CE [V]	CXP [V]
1	339-166	120	53	22	337-250	−75	−30	−9
	339-264		25	22	337-193		−50	−23
	339-222		35	26	337-213		−48	−17
	339-194		43	20	337-293		−22	−13
2	281-123	110	67	12	279-235	−75	−22	−11
	281-206		27	18	279-178		−30	−13
	281-150		47	14	279-100		−18	−13
	281-178		37	16	279-35		−70	−11
3	325-166	120	57	13	323-280	−140	−30	−11
	325-139		77	13	323-220		−48	−9
	325-194		45	13	323-263		−38	−13
	325-282		23	13	323-192		−58	−25
ISTD	381-155	100	35	9	379-279	−145	−36	−13
	381-127		77	9	379-127		−60	−13
	381-77		123	9	379-151		−62	−11
	381-126		113	9	379-277		−66	−17

DP = declustering potential, CE = collision energy, CXP = collision exit cell potential.

either at ambient temperature or at 4 °C. Aliquots were taken and directly frozen at -18 °C on days 0, 3, 6, 10, 13, and 17. They were thawed and mixed with the internal standard directly before analysis by LC-MS/MS.

Test for specificity and ion suppression/enhancement effects

Ten blank urine samples from six healthy male and four female donors, respectively, were prepared, analyzed as described and checked for interfering signals at the expected retention times of the analytes. The effect of the urine matrix on ion suppression and ion enhancement was assessed according to established protocols[19] by post-column split-infusion of analyte mix (1 μg/ml) at a flow rate of 7 μl/min. Five blank urine samples and solvent were subsequently injected into the LC-MS/MS system and tested for matrix effects at the expected retention times of the analytes.

Imprecision

The intra-day imprecision of the method was assessed by analyzing six replicates of fortified urine samples for each analyte at low (2 ng/ml for compounds **1** and **3**, 10 ng/ml for compound **2**), medium (40 ng/ml) and high (200 ng/ml) concentration levels, respectively. The inter-day (or intermediate) imprecision was determined by measuring six replicates at each concentration level on three consecutive days. For each batch of samples, the standard deviation in % defines the imprecision of the method.

Bias

Six replicates at the same concentration levels as described for the imprecision were analyzed and quantified using linear regression of an external calibration curve ranging from 2 to 200 ng/ml for high and medium concentrations, and from 0.5 to 40 ng/ml for the low concentration levels, respectively. The bias was calculated as the ratio (in %) of the determined to the nominal concentrations.

Results and discussion

In vitro metabolism of model HIF stabilizer 1

The metabolic conversion of model HIF stabilizer **1** yielded 3 phase I metabolites (**M1.1** to **M1.3**) and 4 phase II conjugation products (**M1.4** to **M1.7**), as shown in Figure 2 and verified by comparison of the *in vitro* metabolism sample with substrate-, co-factor- and enzyme-blank samples, respectively. Moreover, an unspecific degradation product (**X1**) was observed, which was detected also in the absence of enzymatic activity.

In the initial screening for metabolites, **M1.1** was detected as protonated precursor ion at *m/z* 355 (Figure 2, retention time (RT) = 7.56 min) corresponding to a metabolism-related mass increment (Δ_M) of 16 Da, and according to high resolution/high accuracy MS data (Table 2), to an oxygenation of the active drug. **M1.2** was identified at RT = 7.21 min as a protonated dealkylated product of **1** at *m/z* 297 (Δ_M = -42 Da, $-C_3H_6$, Table 2), while **M1.3** was detected as dehydrogenated cation at *m/z* 337 (Δ_M = -2 Da, $-H_2$, Table 2), co-eluting with the parent compound (*m/z* 339) at 9.45 min.

The intact drug molecule **1** was found to be conjugated with glucuronic acid to yield the phase II metabolites **M1.4** (RT = 6.9 min, Figure 2), **M1.5** and **M1.6** (RT = 8.61/8.73 min, not resolved in Figure 2), all at *m/z* 515 ($+C_6H_8O_6$, Δ_M = +176 Da). Due to the low relative retention on the analytical column with respect to **M1.5/M1.6** and its high relative abundance, **M1.4** is proposed to be glucuronidated at the 4-hydroxy position of the isoquinoline heterocycle, presuming that aromatic hydroxyl groups belong to the most common functions targeted for glucuronic acid conjugation, and that glucuronidation of the carboxy group is expected to decrease the molecular polarity. **M1.5** and **M1.6**, which are not chromatographically resolved in Figure 2 but can be separated using either MRM detection in negative ionization mode (not shown) or the LC high resolution/high accuracy MS system in both positive and negative ion mode (Table 2), are consequently proposed to consist of the acyl-glucuronide and the quaternary

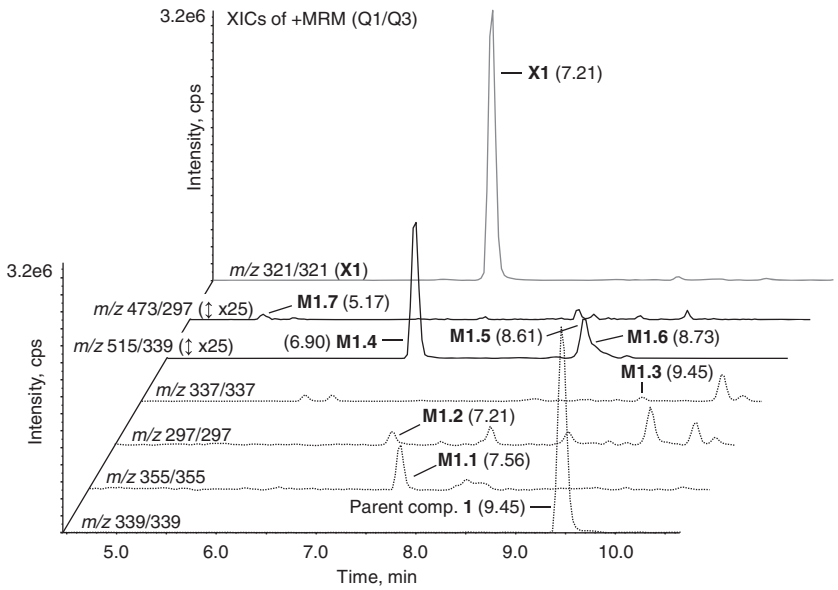

Figure 2. Extracted ion chromatograms (XIC) of an LC-MS/MS analysis of an *in vitro* metabolism sample of model HIF stabilizer **1** (100 μM). Phase I metabolites are depicted as XICs of pseudo-MRM measurements (Q1=Q3, no collisional activation) for unbiased estimation of relative intensities with reduced background noise. For phase II metabolites, the XIC for the collision-induced formation of the aglycone product ion from the protonated precursor (-176 Da) is shown.

Table 2. High resolution / high accuracy MS/HCD-MS data of metabolites of compound **1**

Comp.	Precurs. ions (*m/z*)	Elemental comp.	Error (ppm)	Product ions (*m/z*)	Elemental comp.	Error (ppm)	Cleaved species
[M1.1+H]$^+$	355.0696	$C_{15}H_{16}O_6N_2Cl$	1.2	309.0639	$C_{14}H_{14}O_4N_2Cl$	0.8	CO, H_2O
				298.0481	$C_{13}H_{13}O_5NCl$	1.5	CO, H_2O, CH_2NH, $+H_2O$
				280.0376	$C_{13}H_{11}O_4NCl$	1.8	CO, H_2O, CH_2NH
				240.0061	$C_{10}H_7O_4NCl$	1.3	CO, H_2O, CH_2NH, C_3H_5OH, $+H_2O$
				221.9956	$C_{10}H_5O_3NCl$	1.6	CO, H_2O, CH_2NH, C_3H_5OH
				212.0113	$C_9H_7O_3NCl$	1.8	CO, H_2O, CH_2NH, C_3H_5OH, CO, $+H_2O$
				194.0007*	$C_9H_5O_2NCl$	1.9	CO, H_2O, CH_2NH, C_3H_5OH, CO
				166.0056*	C_8H_5ONCl	1.2	CO, H_2O, CH_2NH, C_3H_5OH, CO, CO
[M1.2+H]$^+$	297.0278	$C_{12}H_{10}O_5N_2Cl$	1.7	251.0221	$C_{11}H_8O_3N_2Cl$	1.3	CO, H_2O
				240.0061	$C_{10}H_7O_4NCl$	1.2	CO, H_2O, CH_2NH, $+H_2O$
				221.9956	$C_{10}H_5O_3NCl$	1.7	CO, H_2O, CH_2NH
				212.0013	$C_9H_7O_3NCl$	1.6	CO, H_2O, CH_2NH, CO, $+H_2O$
				194.0009*	$C_9H_5O_2NCl$	2.8	CO, H_2O, CH_2NH, CO
				166.0056*	C_8H_5ONCl	1.3	CO, H_2O, CH_2NH, CO, CO
[M1.3+H]$^+$	337.0592	$C_{15}H_{14}O_5N_2Cl$	1.8	280.0374	$C_{13}H_{11}O_4NCl$	1.0	CO, H_2O, CH_2NH, $+H_2O$
				262.0271	$C_{13}H_9O_3NCl$	2.2	CO, H_2O, CH_2NH
[X1+H]$^+$	321.1084	$C_{15}H_{17}O_6N_2$	0.8	264.0871	$C_{13}H_{14}O_5N$	1.8	CO, H_2O, CH_2NH, $+H_2O$
				246.0764	$C_{13}H_{12}O_4N$	1.3	CO, H_2O, CH_2NH
				222.0400	$C_{10}H_8O_5N$	1.5	CO, H_2O, CH_2NH, C_3H_6, $+H_2O$
				204.0295	$C_{10}H_6O_4N$	1.9	CO, H_2O, CH_2NH, C_3H_6
				194.0492	$C_9H_8O_4N$	2.2	CO, H_2O, CH_2NH, C_3H_6, CO, $+H_2O$
				176.0345	$C_9H_6O_3N$	1.8	CO, H_2O, CH_2NH, C_3H_6, CO
				148.0396	$C_8H_6O_2N$	1.8	CO, H_2O, CH_2NH, C_3H_6, CO, CO
[M1.4+H]$^+$	515.1073	$C_{21}H_{24}O_{11}N_2Cl$	1.8	339.0745	$C_{15}H_{16}O_5N_2Cl$	0.8	$C_6H_8O_6$
				282.0533	$C_{13}H_{13}O_4NCl$	1.8	$C_6H_8O_6$, CO, H_2O, CH_2NH, $+H_2O$
				264.0424	$C_{13}H_{11}O_3NCl$	0.9	$C_6H_8O_6$, CO, H_2O, CH_2NH
				240.0061	$C_{10}H_7O_4NCl$	1.3	$C_6H_8O_6$, CO, H_2O, CH_2NH, C_3H_6, $+H_2O$
				221.9957	$C_{10}H_5O_3NCl$	1.9	$C_6H_8O_6$, CO, H_2O, CH_2NH, C_3H_6
				212.0110	$C_9H_7O_3NCl$	0.5	$C_6H_8O_6$, CO, H_2O, CH_2NH, C_3H_6, CO, $+H_2O$
				166.0056	C_8H_5ONCl	1.0	$C_6H_8O_6$, CO, H_2O, CH_2NH, C_3H_6, CO, CO
[M1.5+H]$^+$	515.1073	$C_{21}H_{24}O_{11}N_2Cl$	2.0	339.0752	$C_{15}H_{16}O_5N_2Cl$	2.6	$C_6H_8O_6$
				282.0533	$C_{13}H_{13}O_4NCl$	2.1	$C_6H_8O_6$, CO, H_2O, CH_2NH, $+H_2O$
[M1.6+H]$^+$	515.1071	$C_{21}H_{24}O_{11}N_2Cl$	1.5	339.0762	$C_{15}H_{16}O_5N_2Cl$	5.9	$C_6H_8O_6$
[M1.7+H]$^+$	473.0601	$C_{18}H_{18}O_{11}N_2Cl$	1.5	297.0278	$C_{12}H_{10}O_5N_2Cl$	1.8	$C_6H_8O_6$
[M1.2-H]$^-$	295.0135	$C_{12}H_8O_5N_2Cl$	2.6	251.0233	$C_{11}H_8O_3N_2Cl$	1.7	CO_2
				219.981	$C_{10}H_3O_3NCl$	1.3	CO_2, CH_3NH_2
				215.0464	$C_{11}H_7O_3N_2$	1.1	CO_2, HCl
				194.0017	$C_9H_5O_2NCl$	1.4	$C_3H_3NO_3$
				187.0514	$C_{10}H_7O_2N_2$	0.6	CO_2, HCl, CO
				158.0250	$C_9H_4O_2N$	1.4	$C_3H_3NO_3$, HCl
[M1.1-H]$^-$	353.0550	$C_{15}H_{14}O_6N_2Cl$	1.3	309.0656	$C_{14}H_{14}O_4N_2Cl$	2.7	CO_2
				252.0437	$C_{12}H_{11}O_3NCl$	1.7	$C_3H_3NO_3$
				251.02			Overlay of different isotopes
				250.0155	$C_{11}H_7O_3N_2Cl$	1.5	CO_2, C_3H_6OH
				215.0459	$C_{11}H_7O_3N_2$	−1.4	CO_2, C_3H_5OH, HCl
				214.0395	$C_{11}H_6O_3N_2$	−3.5	CO_2, C_3H_6OH, HCl
				213.0307	$C_{11}H_5O_3N_2$	0.6	CO_2, C_3H_6OH, HCl, H
				192.9937	$C_9H_4O_2NCl$	0.7	$C_3H_3NO_3$, C_3H_6OH
				100.0036	$C_3H_2O_3N$	−4.2	$C_{12}H_{12}O_3NCl$
[M1.3-H]$^-$	335.0441	$C_{15}H_{14}O_6N_2Cl$	0.2	291.0543	$C_{14}H_{12}O_3N_2Cl$	0.3	CO_2
				234.0332	$C_{12}H_9O_2NCl$	2.0	$C_3H_3NO_3$

(Continous)

Table 2. *(Continued)*

Comp.	Precurs. ions (*m/z*)	Elemental comp.	Error (ppm)	Product ions (*m/z*)	Elemental comp.	Error (ppm)	Cleaved species
[1-H]⁻	337.0603	$C_{15}H_{14}O_5N_2Cl$	2.4	293.0707	$C_{14}H_{14}O_4N_2Cl$	2.9	CO_2
				251,02		Overlay of different isotopes	
				250.0156	$C_{11}H_7O_3N_2Cl$	2.0	CO_2, C_3H_7
				236.0489	$C_{12}H_{11}O_2NCl$	2.2	$C_3H_3NO_3$
				220.9891*	$C_{10}H_4O_3NCl$	2.8	CO_2, C_3H_7, CH_2NH
				219.9810*	$C_{10}H_3O_3NCl$	1.5	CO_2, C_3H_6, CH_3NH_2
				214.0389	$C_{11}H_6O_3N_2$	2.6	CO_2, C_3H_7, HCl
				213.0309*	$C_{11}H_5O_3N_2$	1.4	CO_2, C_3H_7, HCl, H
				192.9938	$C_9H_4O_2NCl$	1.1	$C_3H_3NO_3$, C_3H_7
				100.0036	$C_3H_2O_3N$	−4.0	$C_{12}H_{12}O_2NCl$
[M1.4-H]⁻	513.0919	$C_{21}H_{22}O_{11}N_2Cl$	0.2	337.0596	$C_{15}H_{14}O_5N_2Cl$	−0.4	$C_6H_8O_6$
				293.0698*	$C_{14}H_{14}O_3N_2Cl$	−0.8	$C_6H_8O_6$, CO_2
				250.0147*	$C_{11}H_7O_3N_2Cl$	0.4	$C_6H_8O_6$, CO_2, C_3H_7
				236.0486*	$C_{12}H_{11}O_2NCl$	−2.1	$C_6H_8O_6$, $C_{12}H_{12}O_2NCl$
				220.9881*	$C_{10}H_4O_3NCl$	−2.0	$C_6H_8O_6$, CO_2, C_3H_7, CH_2NH
				213.0303	$C_{11}H_5O_3N_2$	−1.2	$C_6H_8O_6$, CO_2, C_3H_7, HCl, H
[M1.5-H]⁻	513.0922	$C_{21}H_{22}O_{11}N_2Cl$	0.8	337.0596	$C_{15}H_{14}O_5N_2Cl$	−0.2	$C_6H_8O_6$
				250.0147*	$C_{11}H_7O_3N_2Cl$	−1.4	$C_6H_8O_6$, CO_2, C_3H_7
				213.0305	$C_{11}H_5O_3N_2$	−1.5	$C_6H_8O_6$, CO_2, C_3H_7, HCl, H
[M1.6-H]⁻	513.0920	$C_{21}H_{22}O_{11}N_2Cl$	0.5	337.0599	$C_{15}H_{14}O_5N_2Cl$	−0.6	$C_6H_8O_6$
				293.0693	$C_{14}H_{14}O_3N_2Cl$	−0.7	$C_6H_8O_6$, CO_2
				250.0147*	$C_{11}H_7O_3N_2Cl$	0.6	$C_6H_8O_6$, CO_2, C_3H_7
				220.9883	$C_{10}H_4O_3NCl$	−0.8	$C_6H_8O_6$, CO_2, C_3H_7, CH_2NH
				213.0303	$C_{11}H_5O_3N_2$	−1.4	$C_6H_8O_6$, CO_2, C_3H_7, HCl, H
[M1.7-H]⁻	471.0446	$C_{18}H_{16}O_{11}N_2Cl$	0.4	295.0136	$C_{12}H_8O_5N_2Cl$	2.9	$C_6H_8O_6$,
[X1-H]⁻	319.0933	$C_{15}H_{15}O_6N_2$	−1.0	275.1034	$C_{14}H_{15}O_4N_2$	−1.1	CO_2
				244.0612	$C_{13}H_{10}O_4N$	−1.5	-CO_2, CH_3NH_2
				232.0494	$C_{11}H_8O_4N_2$	1.9	CO_2, C_3H_7
				218.0828	$C_{12}H_{12}O_3N$	2.3	$C_3H_3NO_3$
				202.0144	$C_{10}H_4O_4N$	−1.0	CO_2, C_3H_6, CH_3NH_2
				100.0036	$C_3H_2O_3N$	−4.4	$C_{12}H_{13}O_3N$

MS/MS data recorded at HCD 20;
* HCD 50;

isoquinolonium-*N*-glucuronide, respectively. **M1.7** (RT = 5.17 min) is formed in low abundance and, according to HRMS data, corresponds to a glucuronic acid conjugate of the dealkylated phase I metabolite **M1.2** (Δ_M = 134 Da, -C_3H_6, +$C_6H_8O_6$). A separation and differentiation of theoretically conceivable regioisomers was not achieved for this metabolite. Sulfate conjugates were not detected for this class of compounds using this *in vitro* assay.

The abundant degradation product **X1** (*m/z* 321, RT = 7.21; Figure 2) corresponds to a substitution of the 1-chloro atom by a hydroxyl function (Figure 3), as verified by HRMS-supported determination of the elemental composition (Table 2) and comparison of collision-induced dissociation (CID) pathways with those of compound **1** (*vide infra*).

Characterization of M1 metabolites

Structure confirmation by LC-NMR

The unambiguous identification of metabolite structures of **M1.1** and **M1.2** (Figure 3) was achieved by hyphenated LC-MS-SPE-NMR analysis of the *in vitro* synthesized metabolites and comparison to the earlier reported NMR data of compound **1**.[14]

M1.1: ^{1}H NMR (CD_3OD, 600 MHz), δ (ppm) = 1.39 (3H, d, ^3J = 6.2 Hz, CH_3-10), 3.75-3.77 (2H, m, CH_2-10'), 4.09 (2H, s, CH_2-13), 4.75-4.80 (1H, m, CH-9), 7.54 (1H, dd, $^3J/^4J$ = 9.1/2.4 Hz, CH-6), 7.65 (1H, d, ^4J = 2.4 Hz, CH-8), 8.31 (1H, d, ^3J = 9.. Hz, CH-5). **^{13}C NMR** (CD_3OD, 150 MHz), δ (ppm) = 16.0 (C-10), 42.4 (C-13), 66.0 (C-10'), 108.1 (C-8), 124.6 (C-6), 126.2 (C-5).

M1.2: **^{1}H NMR** (CD_3OD, 600 MHz), δ (ppm) = 3.94 (2H, s, CH_2-11), 7.28 (1H, dd, $^3J/^4J$ = 9.0/2.4 Hz, CH-6), 7.40 (1H, d, ^4J = 2.4 Hz, CH-8), 8.14 (1H, d, ^3J = 9.0 Hz, CH-5). No ^{13}C NMR data available.

CID pathways of M1 metabolites in positive ionization mode

The collision-induced dissociation behaviour of protonated model HIF stabilizers **1** has been thoroughly studied earlier,[14] constituting a valuable basis for the interpretation of product ion mass spectra of the presented protonated metabolites (Figure 4). The most prominent mass spectrometric feature of

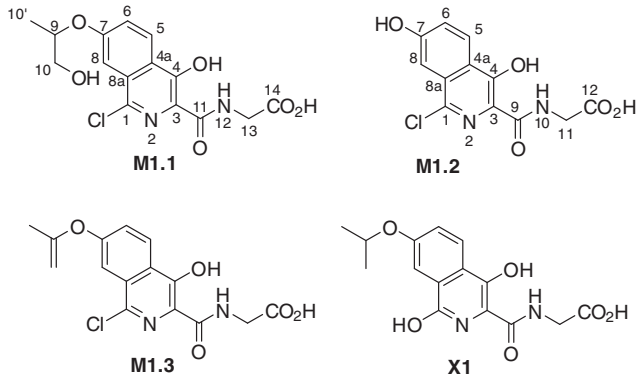

Figure 3. Structures of the phase I metabolites **M1.1** and **M1.2** of HIF stabilizer **1** as confirmed by LC-NMR analysis and the proposed structures of **M1.3** and **X1**, derived from mass spectrometric investigations (see text for further information).

this class of compounds is the spontaneous and reversible ion-molecule reaction between certain types of product ions and residual water in the gas phase, giving rise to unusual, nominal neutral losses of 11 and 10 Da in the course of the dissociation pathway.

These features are also displayed by the analytes identified and discussed here. A generalized scheme of common CID pathways is given in Scheme 1. The main dissociation routes are triggered by losses of water and carbon monoxide, corresponding to losses of −18 Da and 28 Da, respectively (data not shown), from the protonated molecules under formation of methyleneamide product ions, as generalized by structure **I** in Scheme 1a. This ion formally looses a neutral fragment of 11 Da upon MS^3 experiments, which can be explained by an elimination of methyleneamine (-29 Da) generating the isoquinoline-3-acylium product ion (**II**), followed by a spontaneous addition of gas phase water (+18 Da) to form the abundant isoquinoline-3-carboxylic acid product ion **(III)**. This is a phenomenon observed for all phase I metabolites of compound **1** (Scheme 1a).

The differences in the elimination of the alkyl substituent from the isoquinoline heterocycle serve as a good mass spectrometric tool for the identification of the type of metabolic transformation leading to the different phase I metabolites. In case of **M1.1**, the neutral loss of isopropenol (−58 Da) from the acylium product ion at *m/z* 280 (Scheme 1a, **II**), giving rise to the acylium ion at *m/z* 222 (**IV**, mechanism not shown in Scheme 1), indicates a hydroxylation at the isopropoxy moiety. **M1.2**, on the contrary, is lacking the alkyl side chain and the corresponding elimination due to previous metabolic dealkylation, while the indicative ions for the presence of a 1-chloro-dihydroxy-isoquinoline-3-carboxamide core structure (*m/z* 251 [**I**], *m/z* 240 [**III**], *m/z* 222 [**II**, **IV**] etc.) are present in the MS/MS spectrum (Figure 4b and Scheme 1). In case of **M1.3**, the collision-induced dealkylation in the gas phase is strongly disfavoured, arguably due to the metabolic dehydrogenation of the isopropoxy sidechain. Instead, in the MS^3 spectrum of the product ion at *m/z* 262 of **M1.3** (**IV**), a nominal neutral loss of 10 Da is observed, which can be explained by a carbon monoxide elimination (-28 Da) combined with an instant addition of water (+18 Da) to the yield the 1-chloro-3,4-dihydroxy-7-((2-propene)oxy)-isoquinolonium product ion at *m/z* 252 (**VI**). For the active drug molecule as well as the other metabolites, the elimination of the alkyl side chain is a prerequisite for the observation of this neutral loss of 10 Da (Scheme 1b).

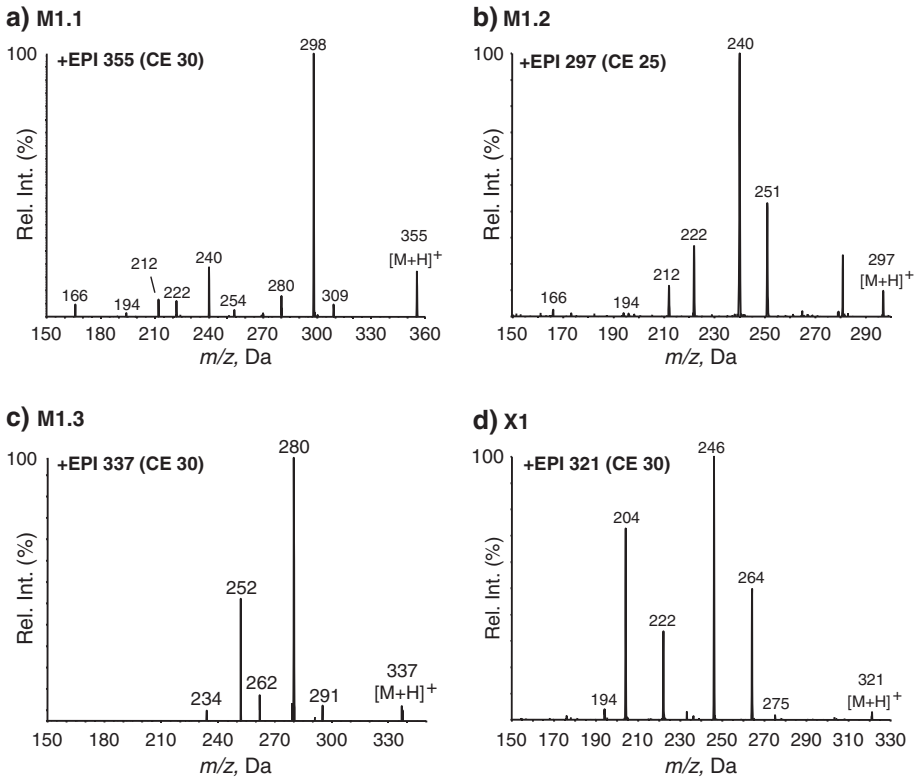

Figure 4. Enhanced product ion spectra (EPI) of protonated metabolites **M1.1**, **M1.2** and **M1.3** and of the degradation product **X1**, recorded by LC-MS/MS analysis of an *in vitro* metabolism sample. Only signals that can unequivocally be attributed to the analyte peak are labelled **(b)**.

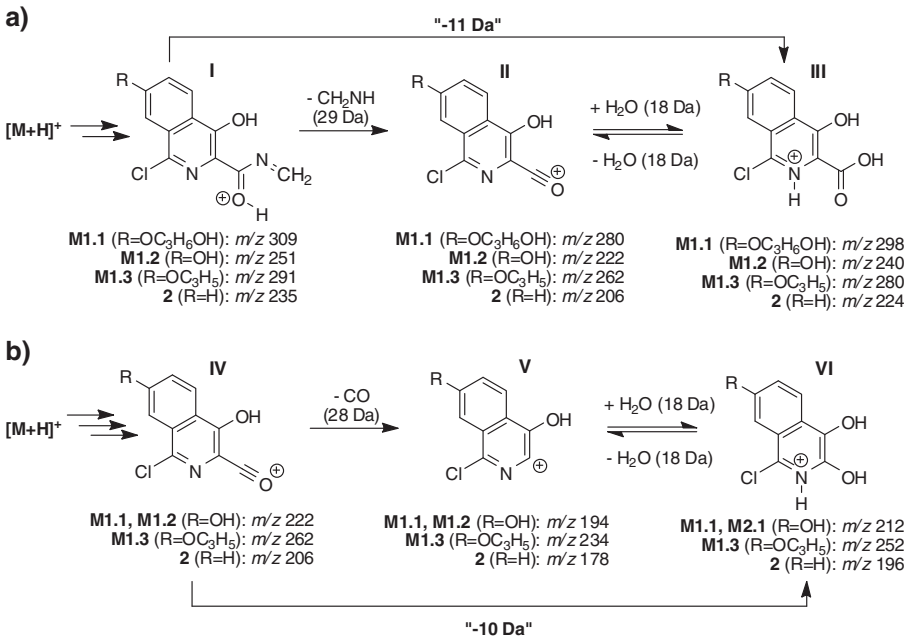

Scheme 1. General collision-induced dissociation pathways of protonated phase I metabolites **M1.1**, **M1.2** and **M1.3** and compound **2**, leading to nominal losses of 11 Da **(a)** and 10 Da **(b)**. In case of **M1.2** and **M1.3**, the structures of the product ions **II** and **IV** are identical. The phase I metabolites of **2** dissociate analogously to **M1.2**. The degradation products **X1** and **X2**, which are not included here, both follow the same dissociation pattern (compare with Table 2).

The dominant collision-induced dissociation pathway of all protonated glucuronides is the formation of the aglycone product ion by elimination of the glucuronic acid moiety (Δ_M = -176 Da, -$C_6H_8O_6$, Table 2). MS^3 experiments employing this aglycone ion as precursor yielded the same spectra as the corresponding unconjugated compound and the phase I metabolite **M1.2**, respectively. All glucuronides were amenable to complete enzymatic hydrolysis by incubation with excess β-glucuronidase for 60 min at 50 °C (not shown).

CID pathways of M1 metabolites in negative ionization mode

Since the scaffold of the presented model HIF stabilizers also exhibits acidic properties, all analytes are also detectable in negative ESI mode. The product ion mass spectra of the deprotonated analytes are shown in Figure 5 and the corresponding accurate masses are listed in Table 2. Scheme 2 depicts the general dissociation behaviour that can be derived from the product ion mass spectra, supported by selective MS^3 experiments (not shown). The most dominant CID reaction for all analytes including compound **1** is the elimination of carbon dioxide (−44 Da) from the carboxylic acid function of the respective precursor ion, yielding a deprotonated isoquinoline-methyleneamide anion at *m/z* 293 in case of **1** (Scheme 2). As substantiated by MS^3 measurements, this ion releases either a propane radical (C_3H_7, -43 Da) or propene (C_3H_6, -42 Da) to yield the product ions at *m/z* 250 or 251, respectively. The radical product ion at *m/z* 250 further eliminates a hydrogen chloride molecule (−36 Da) to produce the ion at *m/z* 214, which eventually looses another hydrogen radical under formation of *m/z* 213. A second general dissociation pathway is triggered by the neutral loss of 2,5-oxazolidinedione ($C_3H_3NO_3$, -101 Da), which is proposed to be formed by cyclization and elimination of the glycineamide moiety, to yield the product ion at *m/z* 236. A subsequent loss of a propane radical (C_3H_7, -43 Da) from the alkyl side chain gives rise to the 1-chloro-4-hydroxy-7-oxy-isoquinoline radical carbanion at *m/z* 193 (Scheme 2, product ion structure not shown).

The product ion formation of the main phase I metabolite **M1.1** follows the same principle pathways as compound **1** but slight differences due to the modified substitution patterns were observed for **M1.2** and **M1.3** (Figure 5 and Scheme 2). The base peak product ion of **M1.2** at *m/z* 251, which is formed by decarboxylation of the deprotonated precursor and constitutes the same isoquinoline-methyleneamide carbanion as in case of compound **1**, eliminates methylamine (-31 Da) giving rise to the product ion at *m/z* 220 (Table 2). Moreover, hydrogen chloride is released from this ion at *m/z* 251 in MS^3 experiments (-36 Da), generating the product ion with *m/z* 215. Generally, the dealkylated metabolite **M1.2** is much less inclined to form radical product ions compared to compound **1** and its main metabolite **M1.1**. The MS/MS spectrum of the deprotonated dehydrogenated metabolite **M1.3** (Figure 5d) is dominated by the product ions at *m/z* 291 and 234, whose structure can be deduced from the analogous ions at *m/z* 293 and 236 of the active drug **1** (Scheme 2). Using more sensitive MRM detection (not shown), signals for the ion transitions 335–250 and 335–193 were observed for **M1.3**, indicating that radical eliminations occur also for this metabolite.

Another general dissociation pathway observed for all analytes is the direct formation of a chloride product ion at *m/z* 35. This is neither listed in the enhanced product ion spectra of Figure 5, nor in the HRMS-data of Table 3, because the ion traps applied in both instrumental setups do not allow for the detection of ions below *m/z* 50. However, using the MS/MS features of the triple quadrupole only (MS^2, MRM), the ion at *m/z* 35 as well as the chloride isotope at *m/z* 37 can be observed after CID of the respective deprotonated precursors (not shown).

The spectra of the deprotonated phase II metabolites **M1.4-M1.7** (not shown) contain the most abundant product ions of the unconjugated analytes, including the aglycone product ions as the dominating ion species. The accurate masses can be found in Table 2.

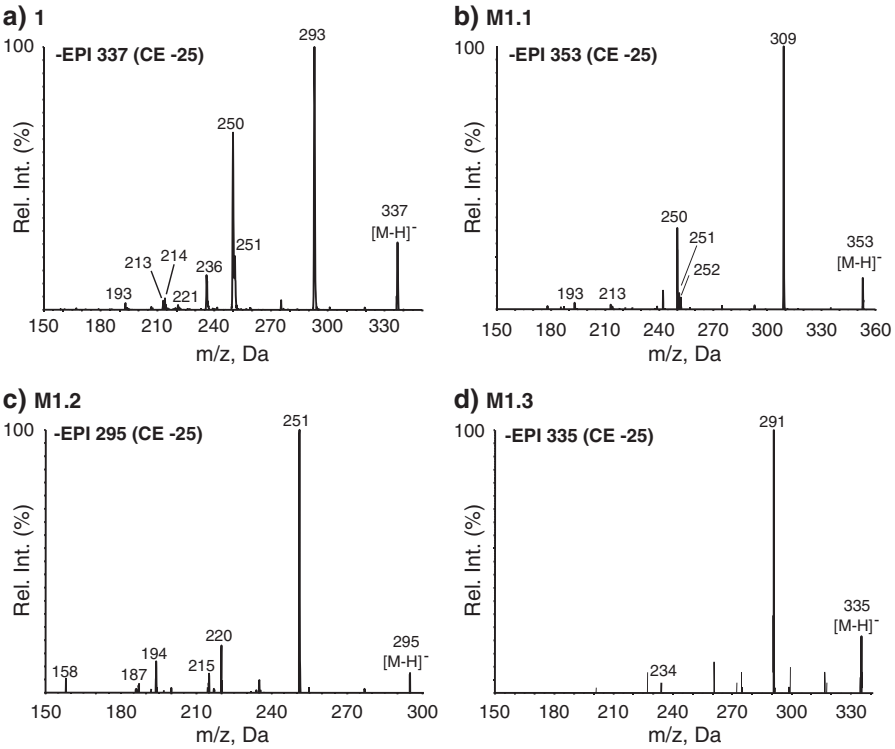

Figure 5. Enhanced product ion spectra of deprotonated compound 1 and its metabolites M1.1, M1.2 and M1.3 obtained by LC-MS/MS analysis. Only signals that can unequivocally be attributed to the analyte peak are labelled.

In vitro metabolism of model HIF stabilizer 2

The *in vitro* investigation of the metabolic fate of model HIF stabilizer **2** yielded a set of hydroxylated metabolites that produce similar MS/MS spectra as the dealkylated metabolite **M1.2** of compound **1**. The corresponding accurate masses of the Exactive MS/MS measurements are given in Table 3. Assisting the interpretation of metabolite formation, the main CID routes for compound **2** after positive and negative ESI, are included in Schemes 1 and 2, respectively.

Following positive ionization of **M2.1** and **M2.2**, the presence of the product ions at *m/z* 222 and *m/z* 240, for example, can serve as reliable diagnostic ions for an hydroxylation at the isoquinoline heterocycle (Scheme 1). However, comparison of

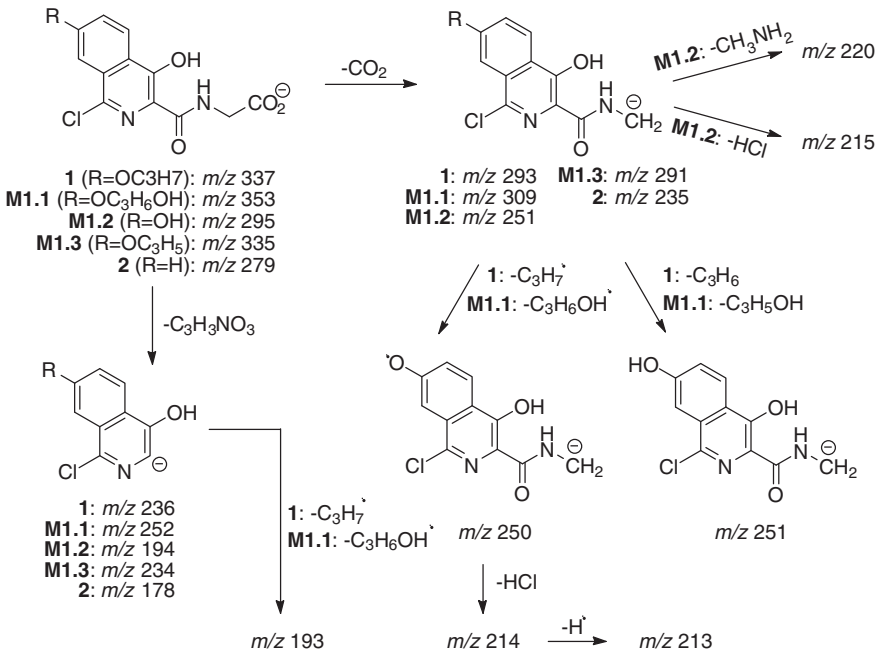

Scheme 2. Proposed fragmentation pathways of compound **1**, its metabolites (**M1.1**, **M1.2**, **M1.3**) and compound **2** as observed after CID of deprotonated molecules.

Table 3. High resolution / high accuracy MS/HCD-MS data of metabolites of compound **2**

Comp.	Precurs. ions(*m/z*)	Elemental comp.	Error (ppm)	Product ions (*m/z*)	Elemental comp.	Error (ppm)	Cleaved species
[M2.1+H]$^+$	297.0269	$C_{12}H_{10}O_5N_2Cl$	−1.4	251.0216	$C_{11}H_8O_3N_2Cl$	−0.8	CO, H_2O
				240.0054	$C_{10}H_7O_4NCl$	−1.5	CO, H_2O, CH_2NH, $+H_2O$
				221.9949	$C_{10}H_5O_3NCl$	−1.6	CO, H_2O, CH_2NH
				166.0053*	C_8H_5ONCl	−0.8	CO, H_2O, CH_2NH, CO, CO
[M2.2+H]$^+$	297.0270	$C_{12}H_{10}O_5N_2Cl$	−0.9	240.0047	$C_{10}H_7O_4NCl$	−4.4	CO, H_2O, CH_2NH, $+H_2O$
				221.9933	$C_{10}H_5O_3NCl$	−8.6	CO, H_2O, CH_2NH
				166.0052*	C_8H_5ONCl	−1.1	CO, H_2O, CH_2NH, CO, CO
[M2.3+H]$^+$	457.0628	$C_{18}H_{18}O_{10}N_2Cl$	−3.5	--			
[M2.4+H]$^+$	473.0573	$C_{18}H_{18}O_{11}N_2Cl$	−4.4	297.0269	$C_{12}H_{10}O_5N_2Cl$	−5.3	$C_6H_8O_6$
[X2+H]$^+$	263.0660	$C_{12}H_{11}O_5N_2$	−0.8	217.0609	$C_{11}H_9O_3N_2$	0.8	CO, H_2O
				206.0445	$C_{10}H_8O_4N$	−1.2	CO, H_2O, CH_2NH, $+H_2O$
				188.0340	$C_{10}H_6O_3N$	−1.0	CO, H_2O, CH_2NH
				178.0497	$C_9H_8O_3N$	1.0	CO, H_2O, CH_2NH, CO, $+H_2O$
				160.0392	$C_9H_6O_2N$	−0.9	CO, H_2O, CH_2NH, CO
				132.0448	C_8H_6ON	3.4	CO, H_2O, CH_2NH, CO, CO
[2-H]$^-$	279.0185	$C_{12}H_8O_4N_2Cl$	2.3	235.0284	$C_{11}H_8O_3N_2Cl$	1.9	CO_2
				178.0066	C_9H_5ONCl	0.6	$C_3H_3NO_3$
				100.0039	$C_3H_2O_3N$	−1.0	$C_9H_6O_1NCl$
[M2.1-H]$^-$	295.0134	$C_{12}H_8O_5N_2Cl$	2.1	251.0234	$C_{14}H_{12}O_3N_2Cl$	1.9	CO_2
				219.9810	$C_{10}H_3O_3NCl$	1.5	CO_2, CH_3NH_2
				187.0514	$C_{10}H_7O_2N_2$	0.6	CO_2, HCl, CO
				158.0244	$C_9H_4O_2N$	−2.5	$C_3H_3NO_3$, HCl
[M2.2-H]$^-$	295.0132	$C_{12}H_8O_5N_2Cl$	1.8	251.0232	$C_{11}H_8O_3N_2Cl$	1.2	CO_2
				219.9810	$C_{10}H_3O_3NCl$	1.3	CO_2, CH_3NH_2
				215.0464	$C_{11}H_7O_3N_2$	0.7	CO_2, HCl
				187.0514	$C_{10}H_7O_2N_2$	0.6	CO_2, HCl, CO
				158.0248	$C_9H_4O_2N$	0.3	$C_3H_3NO_3$, HCl
[M2.3-H]$^-$	455.0512	$C_{18}H_{16}O_{10}N_2Cl$	2.9	279.0188	$C_{12}H_8O_4N_2Cl$	3.7	$C_6H_8O_6$
				235.0282	$C_{11}H_8O_3N_2Cl$	1.0	$C_6H_8O_6$, CO_2
[M2.4-H]$^-$	471.0457	$C_{18}H_{16}O_{11}N_2Cl$	1.9	295.0133	$C_{12}H_8O_5N_2Cl$	2.0	$C_6H_8O_6$
				251.0237	$C_{11}H_8O_3N_2Cl$	3.0	$C_6H_8O_6$, CO_2
				158.0248	$C_9H_4O_2N$	0.5	$C_6H_8O_6$, $C_3H_3NO_3$, HCl
[M2.5-H]$^-$	471.0452	$C_{18}H_{16}O_{11}N_2Cl$	0.7	295.0127	$C_{12}H_8O_5N_2Cl$	−0.1	$C_6H_8O_6$
[X2-H]$^-$	261.0522	$C_{12}H_9O_5N_2$	2.1	217.0621	$C_{11}H_9O_3N_2$	1.3	CO_2
				160.0406	$C_9H_9O_2N$	1.1	$C_3H_3NO_3$
				100.0406	$C_3H_2O_3N$	−1.6	$C_9H_6O_1NCl$

MS/MS data recorded at HCD 20;
* HCD 50; M2.5 was not detected in positive ion mode.

the relative abundances of such specific ion transitions with those of **M1.2** in MRM mode, yielded significantly different ratios as well as slightly different retention times (Figures 6a and 6b). The influence of the aromatic substitution site on the relative intensities of certain product ions have earlier been described for the protonated 6-isopropoxy analogue of compound **1**.[14] This indicates that the hydroxylation of compound **2**, leading to **M2.1** and **M2.2**, is mainly located at positions distinct from the isoquinoline-C7 atom. Due to the chromatographic peak shape depicted in Figure 6b, nonetheless, a mixture of different regioisomers can be assumed in case of **M2.2**.

Evaluation of the MS/MS spectra of the analogous deprotonated precursor ions substantiates the findings in positive ESI mode (spectra not shown, compare HRMS data in Tables 1 and 2). Accordingly, the ratios of diagnostic ion transitions of the hydroxylated metabolites **M2.1** and **M2.2** of compound **2** are significantly different from those of the regioisomeric metabolite **M1.2** (Figures 6d and 6c, respectively). The product ion at *m/z* 215, generated by the loss of hydrogen chloride from the decarboxylated product ion at *m/z* 251, is not observed for the main phase I metabolite **M2.1**. This might be a hint for a hydroxylation at the C8 carbon atom, since this is the most likely position involved in the hydrogen chloride elimination in case of **M2.2**.

In analogy to the phase II metabolism of compound **1**, a glucuronic acid conjugate of unchanged compound **2** is observed at *m/z* 455 (**M2.3**, Table 3, neg. ESI mode), as well as two glucuronides of the hydroxylated phase I metabolites at *m/z* 471 (**M2.4** and **M2.5**). The positions of the glucuronic acid conjugations were not subjected to further investigations at this point.

In accordance to the findings for compound **1**, a dechlorinated and hydroxylated product **X2**, corresponding to a mass loss of 18 Da with respect to the active drug molecule, was detected. The accurate masses of the protonated and deprotonated analyte together with the respective product ions can be found in Table 3.

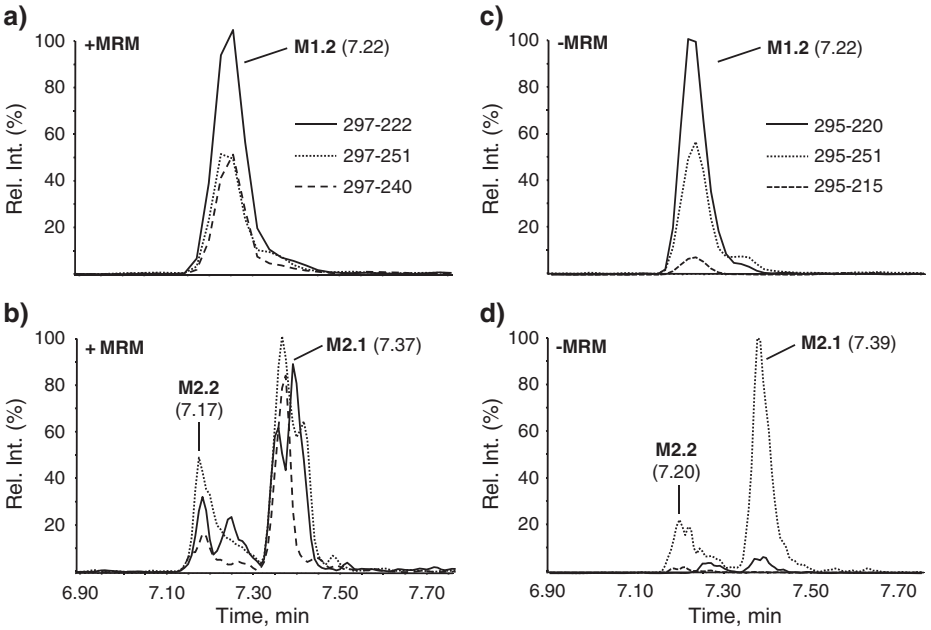

Figure 6. Comparison of relative ion intensities of the different hydroxy-metabolites **M1.2**, **M2.1** and **M2.2**, as detected from *in vitro* metabolism samples of model HIF stabilizers **1** (a, c) and **2** (b, d), in positive and negative MRM mode, respectively.

Analytical assay development

The use of HIF stabilizers in sports has been explicitly banned according to the WADA 2011 Prohibited List.[6] In order to guarantee the detectability of HIF-stabilizing agents that emerge from ongoing clinical trials, reliable screening methods for this class of compounds are needed. The elucidation of the metabolic fate of the two model HIF stabilizers **1** and **2** provides a set of potential target analytes in the LC-MS/MS-based screening for these compounds in urinary doping analysis. Unfortunately, reference material is not yet available for the metabolites described in the previous section. Therefore, new detection assays aiming at these analytes cannot be fully validated but only method characteristics can be defined.

In the course of the metabolite identification work, Bernhardt *et al.* reported on the pharmacokinetics of FG-2216,[20] the first lead drug candidate of Fibrogen and Astellas in the field of HIF-stabilization. In their study, which also included healthy control subjects, a single oral dose of 1250 mg of FG-2216 resulted in plasma drug concentrations of $C_{max} = 179.0 \pm 31.0$ µg/ml and the excretion of $11.0 \pm 3.5\%$ of unchanged FG-2216 into the urine within the first 48 h after the administration. Assuming an excretion of approximately 3000 ml of urine in this time span, this corresponds to a mean urinary FG-2216 concentration of approximately 46 µg/ml. No information concerning the detection of metabolites was presented.

These recently published data suggest that the intact drug molecules can be used as reliable target analytes in a LC-MS/MS detection assay screening for the misuse of HIF stabilizers in urinary doping control analysis. This is especially advantageous, since the compounds **1** and **2**, constituting potential core structures of FG-2216 and related drug candidates, are present as in-house synthesized reference material, thus enabling the setup and validation of an analytical method. For this purpose, a multi-target analytical assay used for routine doping control and based on direct injection of urine into the LS-MS/MS system with detection of analytes in positive and negative MRM mode (scan-to-scan polarity switching), was expanded by diagnostic ion transitions for compounds **1** and **2**. Moreover, the structural analogue **3** (1-chloro-4-hydroxy-6-isopropoxy-isoquinoline-3-carbonyl-N-(2-hydroxyethyl)amide, Figure 1), which was designed as prodrug of the respective [(isoquinoline-3-carbonyl)-amino]-acetic acid, was included into the screening procedure. The previously described $^{13}C_8$-^{15}N-labelled carboxy metabolite of the synthetic cannabinoid JWH-018[16] was used as ampholytic internal standard for both positive and negative MRM detection. For the metabolites listed in the preceding section, the fitness-for-purpose of this method was exemplary verified for three urine samples spiked with *in vitro* metabolite solution (data not shown). Since most HIF stabilizers are not endogenous compounds, a qualitative determination of these substances in human urine would be sufficient for reporting a doping control sample as positive. Nevertheless, a full validation procedure for the quantitative detection of compounds **1–3** was carried out according to common guidelines, in order to illustrate the applicability of this method to other analytical fields like clinical or forensic drug testing.

Validation

In the course of the validation process, the negative ionization mode proved to be superior to the detection of protonated analytes, both in terms of assay sensitivity and precision. Therefore, the full evaluation of the data is only presented for the deprotonated analytes. A summary is given in Table 4.

The stability of analytes in urine matrix proved to be critical to the storage conditions. While complete degradation of all analytes within 10 days was observed after storage of spiked urine samples at room temperature, no significant stability effects were observed when the samples were stored at 4 °C. Similar results were obtained, after storage of the analytes in blank MilliQ water, indicating non-enzymatic degradation processes to be

Table 4. Method validation results for compounds **1–3**

Compound	LLOD [ng/ml]	LLOQ [ng/ml]	Conc. [ng/ml]	Imprecision [%]			Bias [%]		
				2/10*	40	200	2 (10)	40	200
1	0.8	2.0	Intraday (n=6+6+6)	12.2	7.8	8.6	102	94	101
			Interday (n=18+18+18)	19.6	16.6	10.3			
2	10	10[#]	Intraday (n=6+6+6)	9.4*	5.8	6.3	99*	97	100
			Interday (n=18+18+18)	11.4*	17.0	13.5			
3	0.6	2.0	Intraday (n=6+6+6)	12.6	6.9	10.3	103	100	103
			Interday (n=18+18+18)	12.9	16.0	10.3			

[#] refer to the text for explanation;

* The lowest conc. level for comp. **2** was 10 ng/ml

responsible for the destruction of the analytes. Interestingly, the degradation can be avoided, if the samples are stored in 2% aqueous acetic acid solution. With regard to routine doping control procedures, a cooled transport and either immediate processing or refrigerated storage of the samples (4 °C or -18 °C) are the preferred ways of sample processing and expected to be sufficient to ensure a reliable analysis of A- and B-samples. The test for ion suppression/enhancement effects by post column split-infusion of analytes yielded no significant matrix effects on the extracted ion chromatograms of the analytes **1–3**. The linearity test of the detection assay was conducted between 2 and 200 ng/ml and yielded coefficients of correlation > 0.99 for all 3 analytes.

The method showed specificity as no interfering signals were observed for the selected ion transitions at the retention times of the target compounds in (Figure 7). For the most intense ion transition of deprotonated compound **2** (*m/z* 279–235, Tables 1 and 3) however, the blank chromatograms show significant background noise due to matrix interferences (not shown). Therefore, the transition *m/z* 279–178 is proposed to serve as major screening tool for this compound. The relatively high estimated LLOD ($S/N \leq 3$) of approximately 10 ng/ml is due to the small number of abundant diagnostic product ions for deprotonated **2** and consequently, unequivocal compound identification needs to rely on the low intensity *m/z* 279–100 as third diagnostic ion transition. Additionally, the ion transitions of the ^{37}Cl isotope of deprotonated **2** (e.g. *m/z* 281–180) or ions derived from positive ESI might be considered for supportive identification purposes (not accounted for, here). For the ion transition *m/z* 279–178, which proved to be the most reliable also for quantification, a signal-to-noise ratio of approximately 25 can be calculated at 10 ng/ml. Therefore, the LLOQ (requiring an S/N of "only" 10) was chosen to be set at the same concentration level as the LLOD for compound **2** (Table 4).

The intraday imprecision (or repeatability) as well as the interday (or intermediate) imprecision was calculated below 20% for all analytes at the LLOQ (2 ng/ml for **1** and **3**, 10 ng/ml for **2**), intermediate (40 ng/ml) and high (200 ng/ml) concentration levels, respectively. Moreover, the bias of the method was found between 94 and 103% for all analytes (Table 4).

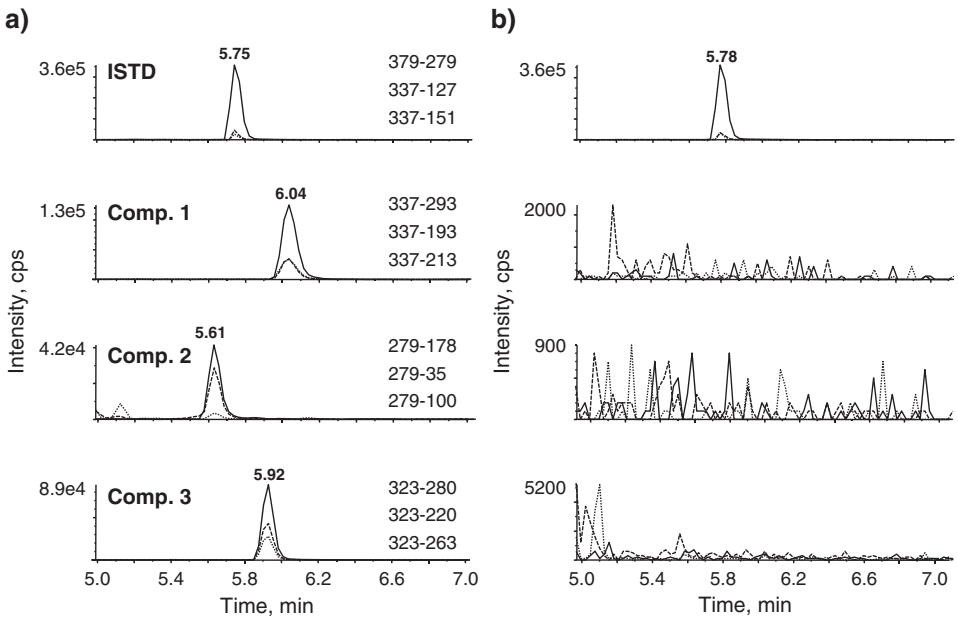

Figure 7. Extracted ion chromatograms of an LC-MS/MS analysis of **a)** blank urine sample spiked with internal standard (50 ng/ml) and compounds **1**, **2** and **3** (40 ng/ml), and **b)** blank urine spiked with internal standard only.

Alternative LC-MS/MS-approaches for screening procedures

As presented in the previous chapter, the LC-MS/MS-based detection assay using MRM of diagnostic product ions of the deprotonated compounds **1–3** constitutes a sensitive, precise and highly selective tool for a targeted screening. However, a profound challenge for preventive doping control is the fact that exact molecular structures of the drug candidates are often undisclosed in the early clinical stages. This also applies to FG-2216, currently the most advanced HIF stabilizer in clinical tests. Moreover, new structural analogues with improved drug properties often emerge in the course of clinical investigations (like FG-4592). This lack of information and the constant structural development require more comprehensive detection assays, enabling also the determination of structural analogues that would be missed by selective MRM methods. In a previously reported example of preventive doping analysis, a screening for unknown designer steroids was realized by applying the precursor ion scan mode of triple quadrupole mass spectrometers.[21] Following the same analytical approach, the uniform dissociation characteristics of this class of compounds after positive electrospray ionization offer various potential diagnostic ions. The abundant product ion with *m/z* 166, for instance, is observed after high energy CID of compound **1** and **3**, as well as all metabolites of **1**. It is formed by carbon monoxide elimination (-28 Da) from the 1-chloro-dihydroxyisoquinoline carbenium product ion with *m/z* 194 (compare Scheme 1, Table 2 and reference 14) and serves as diagnostic ion for a chloro- and di-hydroxy-substituted isoquinoline heterocycle. Consequently, a precursor ion scan for *m/z* 166 is descriptive for HIF stabilizers **1** and **3**, providing LODs (S/N≥3) of approximately 90 and 20 ng/ml, respectively (Figure 8, a1 and a2). Moreover, this scan mode allows for the detection of the hydroxylated metabolite **M2.1** of compound **2** from *in vitro* metabolite solutions (Figure 8, a3).

Even more comprehensive than the precursor ion scan for certain product ions is a neutral loss scan for the unusual nominal elimination of 10 Da, which is observed for all protonated phase I metabolites described here (Scheme 1b). In order to detect this phenomenon with such a scan mode, the acylium product ions, constituting the precursors for the combined gas phase

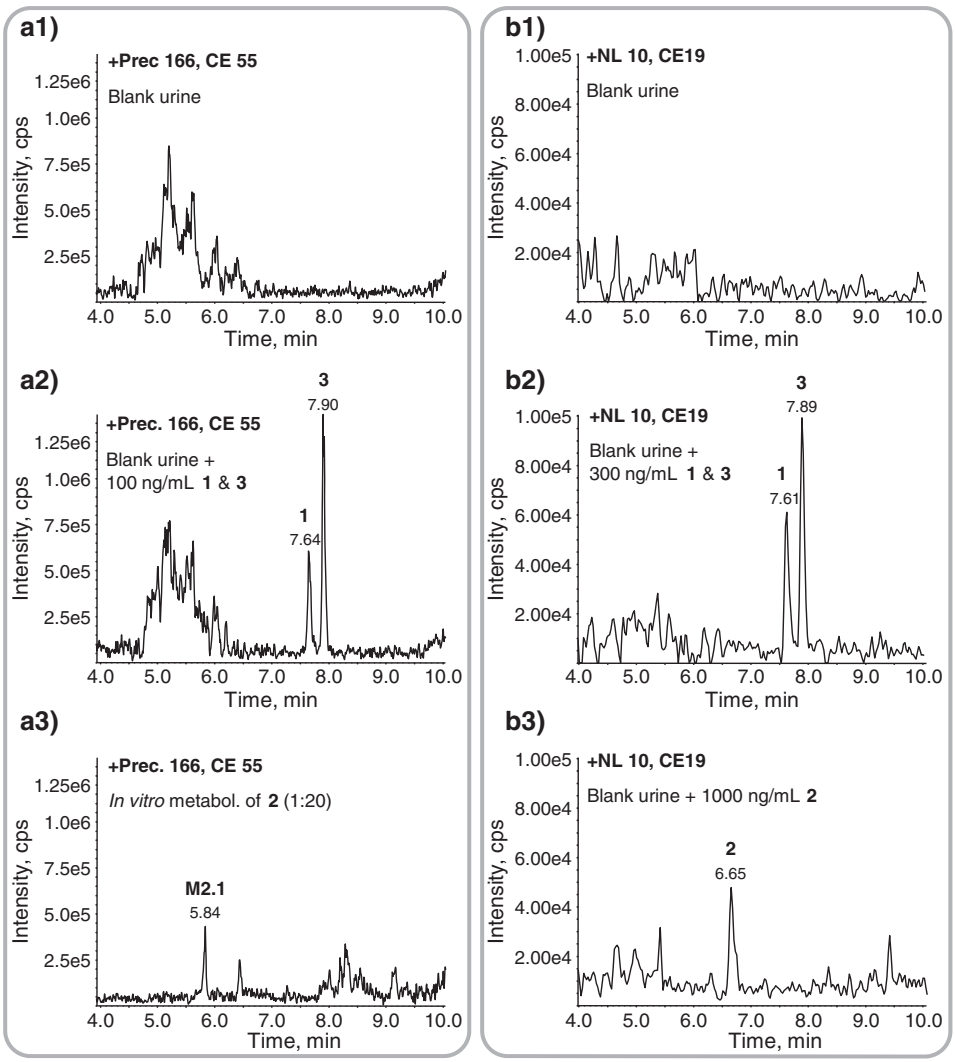

Figure 8. Blank urine sample **(a1)**, blank urine spiked with 100 ng/ml of compounds **1** and **3 (a2)** and *in vitro* incubation sample of 2 **(a3)** analyzed by direct injection LC-MS/MS in precursor ion scan mode. Neutral loss scan was conducted with direct injection of blank urine sample **(b1)**, blank urine spiked with 300 ng/ml of compounds **1** and **3 (b2)** and blank urine spiked with 1000 ng/ml of **2 (c)** (chromatograms were smoothed and background subtracted).

elimination/ion-molecule reaction, have to be generated prior to their entering the first quadrupole of the MS-system. On the API 5500 QTrap system, a declustering potential of 220 V proved to be ideal for the formation of the desired ions by nozzle-skimmer (in-source) CID of protonated precursors. A range from *m/z* 110 to 400 was scanned at a rate of 200 Da/s, resulting in a cycle time of 1.5 s. The slow scan rate was found to be crucial for the sensitivity of the scan. Moreover, the resolution of the two quadrupoles Q1 and Q3 was set to unit and low resolution, respectively, exerting a similar beneficial influence on the sensitivity. As seen in Figure 8b, a direct injection LC-MS/MS analysis with a spiked urine sample containing 300 ng/ml of HIF stabilizers **1** and **3** and 1000 ng/ml of **2** yields reliable signals for all analytes with S/N ratios of approximately 6, 10, and 4, respectively. The gradient runtime for both the neutral loss and the precursor ion scan was extended from 4 to 8 min, in order to ensure a sufficient chromatographic separation of analytes.

The neutral loss scan for 10 Da reliably detects analytes comprising an isoquinoline-3-carboxamide scaffold, independent from changes in the substitution pattern, both on the heterocycle as well as the carboxamide moiety. For this reason, it can serve as analytical tool to determine the most potent HIF stabilizers developed by Fibrogen, based on isoquinoline-3-carboxamide core structures, even though the definite compositions are not yet officially confirmed. The LC-MS scan also detects the phase I metabolites presented in this work (not shown) as well as potentially unknown metabolites. Structurally related pyridine carboxamides, which are also investigated as HIF stabilizers by Fibrogen and other pharmaceutical companies,[7] are very likely to be covered by the same analytical approach. This however, cannot be verified at the moment due to the lack of reference material. Moreover, the neutral loss of 10 Da has also been observed for a set of structurally unrelated xenobiotic substances, like the synthetic cannabinoids JWH-018, its metabolites and structural analogues.[16] On the one hand, this expands the list of prohibited, potential target analytes covered by this approach; on the other hand, this increases the possibility of interferences, arising from endogenous or non-prohibited exogenous sources (e.g. nutrition).

No abundant interfering signals in the retention time window from 2 to 12 min were observed after direct-injection-LC-MS/MS analysis of 10 blank urine samples and 40 doping control samples that were reported negative in the course of the routine screening procedure. However, due to the noisy background, it is recommended to neglect peaks with a signal-to-noise below 5. Moreover, numerous intense signals were detected at or close to the retention time of the injection peak, indicating a strong influence of the urine matrix on the detection of early eluting compounds. If implemented into routine doping control procedures, it would be advisable to analyze a larger batch of blank urine samples and to create an exclusion list for possible interfering signals from urine matrix. Since the scan is based on in-source-generated product ions (pseudo MS^3), a precursor ion scan for the ion reporting the neutral loss has to be conducted for the determination of the corresponding quasi-molecular ion. In a second step, this ion can be characterized by means of MS/MS for potential confirmatory analyses.

Noteworthy, the alternative approaches, both the neutral loss as well as the precursor ion scan, cannot compete with the sensitivity usually achieved for targeted analytical assays, using for instance MRM-detection. However, this is regarded as a maintainable trade-off for the increased comprehensiveness of the method, especially considering the high urinary concentrations that are to be expected after therapeutic dosages of FG-2216, ranging between 375 and 1250 mg twice or three times a week.[20,22]

Conclusion

In the 2011 Prohibited List, WADA categorized HIF stabilizers as an erythropoiesis-stimulating agent under paragraph S2.1 (peptides, growth hormones and related substances) and explicitly banned their use in sports.[6] Here, we report the first validated LC-MS/MS-based analytical assay for the determination of investigational HIF stabilizers like FG-2216 in human urine, the most frequently used matrix in doping control analysis. The data regarding the metabolic fate of model HIF stabilizers **1** and **2** may be useful for potential confirmation analyses and the determination of possible long-term urinary metabolites in the future. The LC-MS/MS scan for a neutral loss of 10 Da constitutes a comprehensive approach for the screening for structure-related HIF stabilizers with yet unknown molecular composition, like the second generation HIF-PHI FG-4592.

To the best of our knowledge, no evidence for a circulation or even misuse of HIF stabilizers amongst elite or amateur athletes has been obtained so far. However, the experience of sports drug testing showed several cases where clinically unapproved, performance-enhancing substances were available via the Internet[23] and/or were suspected to be misused as doping agents in sports[24] before their pharmaceutical launch. In the case of HIF stabilizers, every athlete intending to cheat with this novel class of doping agent takes a hazardous risk: numerous concerns about the selectivity and long-term effects of HIF-PHD inhibition have been raised by experts.[1,25] For instance, prolyl hydroxylases not only play a central role in the HIF signalling pathway but are involved in the regulation of numerous other proteins like the transcription factor NF-κB, promoting cell survival during tumour growth.[26] Such concerns will have to be addressed in the ongoing development of the therapeutic use of HIF-PHIs and, hopefully, will exert a deterrent influence on intentional misuse. Should HIF stabilizers, regardless of the abovementioned objections, become an issue in sports in the future, the piece of preventive doping research presented here allows the early detection of such novel performance-enhancing agents in doping control analysis.

Acknowledgments

The project was conducted with support of Antidoping Switzerland (Berne, Switzerland), the German Federal Ministry of the Interior (Berlin, Germany) and the Manfred-Donike Institute for Doping Analysis (Cologne, Germany).

References

[1] T. Tanaka, M. Nangaku. Drug discovery for overcoming chronic kidney disease (CKD): prolyl-hydroxylase inhibitors to activate hypoxia-inducible factor (HIF) as a novel therapeutic approach in CKD. *J. Pharmacol. Sci.* **2009**, *109*, 24.

[2] K. Bruegge, W. Jelkmann, E. Metzen. Hydroxylation of hypoxia-inducible transcription factors and chemical compounds targeting the HIF-alpha hydroxylases. *Curr. Med. Chem.* **2007**, *14*, 1853.

[3] P. Urquilla. Upregulation of endogenous EPO in healthy subjects by inhibition of HIF-PH. *J. Am. Soc. Nephrol.* **2004**, *15*, 546A.

[4] A. Besarab, H. N. Hulter, S. Klaus, T. T. Lee, D. E. Lilienfeld, T. Neff, B. A. Piper, A. Provenzano, P. K. Yu. FG-4592, A novel oral HIF prolyl hydroxylase inhibitor, elevates hemoglobin in anemic stage 3/4 CKD patients. *J. Am. Soc. Nephrol.* **2010**, *21*, 95A.
[5] R. K. Bruick, S. L. McKnight. A conserved family of prolyl-4-hydroxylases that modify HIF. *Science* **2001**, *294*, 1337.
[6] WADA (World Anti-Doping Agency). The 2011 Prohibited List. Available at: http://www.wada-ama.org/Documents/World_Anti-Doping_Program/WADP-Prohibited-list/To_be_effective/WADA_Prohibited_List_2011_EN.pdf [18 August 2011].
[7] L. Yan, V. J. Colandrea, J. J. Hale. Prolyl hydroxylase domain-containing protein inhibitors as stabilizers of hypoxia-inducible factor: small molecule-based therapeutics for anemia. *Expert Opin. Ther. Pat.* **2010**, *20*, 1219.
[8] Fibrogen Inc. FibroGen Announces Initiation of Phase 2b Studies of FG-4592, an Oral HIF Prolyl Hydroxylase Inhibitor, for Treatment of Anemia in Chronic Kidney Disease. Available at: http://www.fibrogen.com/press/release/pr_1300378657 [5 May 2011].
[9] Fibrogen Inc. FibroGen Licenses Oral HIF-PH Inhibitors, Including FG-2216 and FG-4592, to Astellas for the Treatment of Anemia in Europe and Other Regions. Available at: http://www.fibrogen.com/press/release/pr_1210878669 [31 May 2011].
[10] S. Philipp, J. S. Jürgensen, J. Fielitz, W. M. Bernhardt, A. Weidemann, A. Schiche, B. Pilz, R. Dietz, V. Regitz-Zagrosek, K. U. Eckardt, R. Willenbrock. Stabilization of hypoxia inducible factor rather than modulation of collagen metabolism improves cardiac function after acute myocardial infarction in rats. *Eur. J. Heart Fail.* **2006**, *8*, 347.
[11] Fibrogen. Novel nitrogen-containing heteroaryl compounds and methods of use thereof. US Patent No. 20040254215A1, **2004**.
[12] Fibrogen Inc. Treatment method for anemia. US Patent No. 20060276477A1, **2006**.
[13] M. Thevis, M. Kohler, N. Schlörer, W. Schänzer. Gas phase reaction of substituted isoquinolines to carboxylic acids in ion trap and triple quadrupole mass spectrometers after electrospray ionization and collision-induced dissociation. *J. Am. Soc. Mass Spectrom.* **2008**, *19*, 151.
[14] S. Beuck, T. Schwabe, S. Grimme, N. Schlörer, M. Kamber, W. Schänzer, M. Thevis. Unusual mass spectrometric dissociation pathway of protonated isoquinoline-3-carboxamides due to multiple reversible water adduct formation in the gas phase. *J. Am. Soc. Mass Spectrom.* **2009**, *20*, 2034.
[15] S. Guddat, E. Solymos, A. Orlovius, A. Thomas, G. Sigmund, H. Geyer, M. Thevis, W. Schänzer. High-throughput screening for various classes of doping agents using a new 'dilute-and-shoot' liquid chromatography / tandem mass spectrometry multi-target approach. *Drug Test. Analysis* **2011**, *3*, this issue.
[16] S. Beuck, I. Möller, A. Thomas, A. Klose, N. Schlörer, W. Schänzer, M. Thevis. Structure characterisation of urinary metabolites of the cannabimimetic JWH-018 using chemically synthesised reference material for the support of LC-MS/MS-based drug testing. *Anal. Bioanal. Chem.* **2011**, DOI:10.1007/s00216-011-4931-5
[17] T. Kuuranne, A. Leinonen, W. Schänzer, M. Kamber, R. Kostiainen, M. Thevis. Aryl-propionamide-derived selective androgen receptor modulators: liquid chromatography-tandem mass spectrometry characterization of the in vitro synthesized metabolites for doping control purposes. *Drug Metab. Dispos.* **2008**, *36*, 571.
[18] M. Thevis, I. Möller, A. Thomas, S. Beuck, G. Rodchenkov, W. Bornatsch, H. Geyer, W. Schänzer. Characterization of two major urinary metabolites of the PPARdelta-agonist GW1516 and implementation of the drug in routine doping controls. *Anal. Bioanal. Chem.* **2010**, *396*, 2479.
[19] B. K. Matuszewski, M. L. Constanzer, C. M. Chavez-Eng. Strategies for the assessment of matrix effect in quantitative bioanalytical methods based on HPLC-MS/MS. *Anal. Chem.* **2003**, *75*, 3019.
[20] W. M. Bernhardt, M. S. Wiesener, P. Scigalla, J. Chou, R. E. Schmieder, V. Günzler, K. U. Eckardt. Inhibition of prolyl hydroxylases increases erythropoietin production in ESRD. *J. Am. Soc. Nephrol.* **2010**, *21*, 2151.
[21] M. Thevis, H. Geyer, U. Mareck, W. Schänzer. Screening for unknown synthetic steroids in human urine by liquid chromatography-tandem mass spectrometry. *J. Mass Spectrom.* **2005**, *40*, 955.
[22] R. Provenzano, G. Fadda, M. Bernardo, C. James, G. Kochendoerfer, T. Lee, T. Neff, R. H. Ellison, B. A. Piper. FG-2216, A novel oral HIF-PHI, stimulates erythropoiesis and increases hemoglobin concentration in patients with non-dialysis CKD. *Am. J. Kidney Dis.* **2008**, *51*, B80.
[23] M. Thevis, H. Geyer, M. Kamber, W. Schänzer. Detection of the arylpropionamide-derived selective androgen receptor modulator (SARM) S-4 (Andarine) in a black-market product. *Drug Test. Analysis* **2009**, *1*, 387.
[24] P. Benkimoun. Police find unlicensed drugs after trawling bins. *BMJ* **2009**, *339*, b4201.
[25] H. F. Bunn. New agents that stimulate erythropoiesis. *Blood* **2007**, *109*, 868.
[26] E. P. Cummins, E. Berra, K. M. Comerford, A. Ginouves, K. T. Fitzgerald, F. Seeballuck, C. Godson, J. E. Nielsen, P. Moynagh, J. Pouyssegur, C. T. Taylor. Prolyl hydroxylase-1 negatively regulates IkappaB kinase-beta, giving insight into hypoxia-induced NFkappaB activity. *P. Natl. Acad. Sci. USA* **2006**, *103*, 18154.